

Improved Fueling and Transport Barrier Formation with Pellet Injection from Different Locations on DIII-D*

L.R. Baylor¹, T.C. Jernigan¹, P. Gohil², G.L. Schmidt³, K. H. Burrell², S.K. Combs¹,
D.R. Ernst³, C.M. Greenfield², R.J. Groebner², W.A. Houlberg¹, C. Hsieh², M. Murakami¹,
P.B. Parks², M. Porkolab⁴, W.D. Sessions⁵, G.M. Staebler², E.J. Synakowski³,
and the DIII-D TEAM

¹*Oak Ridge National Laboratory, Oak Ridge, TN, USA*

²*General Atomics, San Diego, CA, USA*

³*Princeton Plasma Physics Laboratory, Princeton, NJ, USA*

⁴*Massachusetts Institute of Technology, Cambridge, MA, USA*

⁵*Tennessee Technological University, Cookeville, TN, USA*

e-mail contact of main author: baylorlr@ornl.gov

Abstract

Pellet injection has been employed on DIII-D from different injection locations to optimize the mass deposition for density profile control and internal transport barrier formation. Transport barriers have been formed deep in the plasma core with central mass deposition from high field side (HFS) injected pellets and in the edge with pellets that trigger L-mode to H-mode transitions. Pellets injected from all locations can trigger the H-mode transition, which depends on the edge density gradient created and not on the radial extent of the pellet deposition. Pellets injected from inside the magnetic axis from the inner wall or vertical port lead to stronger central mass deposition than pellets injected from the low field side (LFS) and thus yield deeper more efficient fueling.

1. Introduction

Recent experiments on the DIII-D tokamak have been performed with pellet injection to study fueling and transport barrier formation. The injector used has three independent barrels that allow for a comparison of the fueling from different injection locations in the same discharges. Injection ports have been installed with the use of curved guide tubes on the inner wall and vertical access ports as shown in Fig. 1.

In this paper we discuss comparisons that have been made of the fuel deposition and fueling efficiency from the different pellet injection locations. The density perturbations from the pellets have been used to form internal transport barriers (ITBs) and trigger L-mode to H-mode transitions. Deep fueling from the high field side (HFS) injection ports helps to form the ITBs when negative central magnetic shear (NCS) or low central magnetic shear (LS) is present near the magnetic axis.

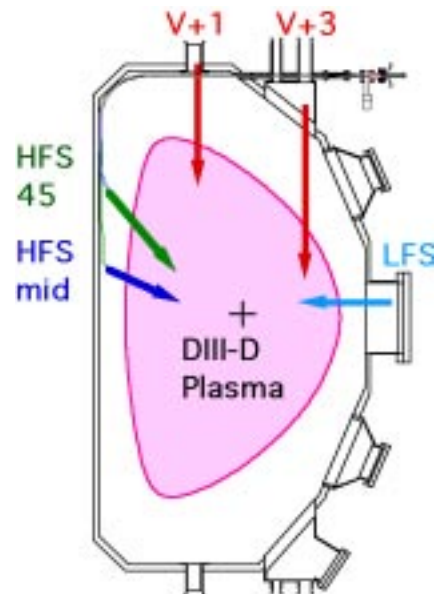


FIG. 1. The five separate pellet injection locations on DIII-D shown in a poloidal cross section.

* Work supported by U.S. Department of Energy under Contracts DE-AC05-96OR22464, DE-AC03-99ER54463, and DE-AC02-76CH03073.

The L-mode to H-mode transition is triggered by pellets injected from all locations and thus does not depend on the radial extent of the fuel deposition.

2. Fueling Comparison

Pellets injected from the HFS lead to deeper mass deposition than identical pellets injected from the outside midplane, in spite of a factor of four lower pellet speed [1] as is shown in Fig.2. This improvement in deposition with HFS pellet injection agrees with the original observation of improved fueling efficiency from ASDEX-Upgrade [2]. The deeper mass deposition observed for the slow HFS pellets suggests that moderate velocity HFS launched pellets may provide a solution to refueling a high-temperature tokamak reactor plasma. Accurate measurements of the pellet deposition profile indicate that a strong major radius drift appears to play a role in the fueling from all five injection locations on DIII-D. The mechanism is hypothesized to be an EXB force on the vertically polarized ablatant that occurs from curvature and ∇B drifts of the ions and electrons in the dense pellet ablatant cloud. Modeling of the mass deposition using a recently developed polarization induced drift model [3] gives qualitative agreement with the measured deposition. Improvements to the model are underway to include local profile effects that promise to enhance the quantitative agreement with the experimental data.

A comparison of pellet deposition from the two vertical injection ports in similar discharges indicates deeper mass deposition for the V+1 port than the V+3 port as shown in Fig. 3. The V+1 pellet deposition shows deep penetration inside the tangency radius of the port while the V+3 pellet mass is largely deposited well outside the tangency radius. An outward drift of the pellet mass in the major radius direction is consistent with the difference in the resulting deposition profiles.

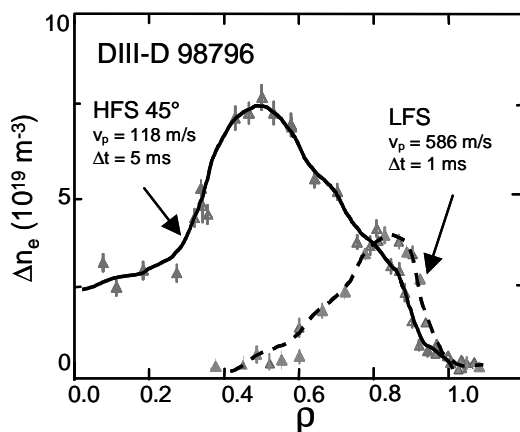


FIG. 2. Comparison of deposition profiles for a 2.7mm HFS pellet and LFS pellet in the same discharge.

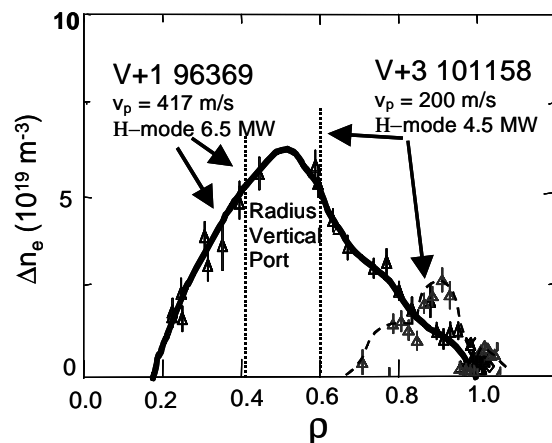


FIG. 3. Comparison of deposition profiles for a 2.7mm V+1 pellet and V+3 pellet in similar H-mode discharges.

Pellets injected into H-mode plasmas from all locations are found to trigger edge localized modes (ELMs) [4] presumably due to pellet induced changes in edge stability [5]. ELMs triggered from the low field side (LFS) outside midplane injected pellets are of significantly larger amplitude and longer duration than from HFS injected pellets. The rapid loss of particles from the outward major radius drift of the pellet ablatant may be partially responsible for the stronger ELMs induced by LFS injected pellets.

The fueling efficiency from the different pellet injection locations has been analyzed using the density profiles measured immediately after injection. LFS pellet injection in ELMing H-mode plasmas has a relatively low fueling efficiency of ~50% due to the pellet induced ELM that ejects a sizeable portion of the edge density pedestal. HFS pellet injection has a nearly ideal fueling efficiency of ~90% in ELMing H-mode, which is much higher than LFS injection due to deeper mass penetration and a reduced ELM perturbation [4]. The V+1 vertical injection has a fueling efficiency in between the LFS and HFS injected pellets.

3. Transport Barrier Formation

Deep HFS pellet fueling during the plasma current rise in combination with co- or counter-neutral beam injection (NBI) leads to the formation of an ITB that is similar to the pellet enhanced performance (PEP) -mode obtained on JET [6]. The HFS injected pellets generate peaked density profile plasmas with a peaking factor $n_e(0)/\langle n_e \rangle$ in excess of 3 that develop ITBs when centrally heated with NBI. The resulting profiles after ITB formation are shown for two cases in Fig.4. The transport barrier is formed in conditions where $T_e \sim T_i$ and $q(0)$ is above unity, unlike other ITB plasmas on DIII-D where $T_i \gg T_e$ [7,8]. The peaked density profiles, characteristic of the internal transport barrier, persist for several energy confinement times. The normalized beta (β_N) is approximately 1.5 for these PEP discharges due to only 15% of the plasma volume being inside the ITB.

These DIII-D PEP experiments are the first to use only NBI heating and the first with the radial electric field determined. Strong off-axis bootstrap current generated by a sharp pressure gradient modifies the q profile, which can sustain a very strong negative shear region in the plasma core. Thermal transport is reduced in the core negative shear region similar to non-PEP ITB plasmas and is consistent with $\mathbf{E} \times \mathbf{B}$ shear suppression of ITG modes. Electron particle transport is reduced more strongly in the core than in non-PEP ITB plasmas.

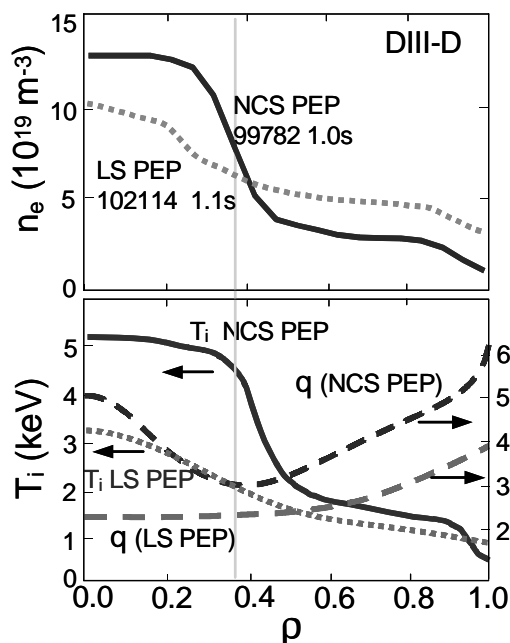


FIG. 4. Profiles of n_e , T_i , and q for pellet induced ITB (NCS PEP) plasma and low shear ITB (LS PEP). The strong gradients for the NCS PEP are just inside the minimum in the q profile (vertical line).

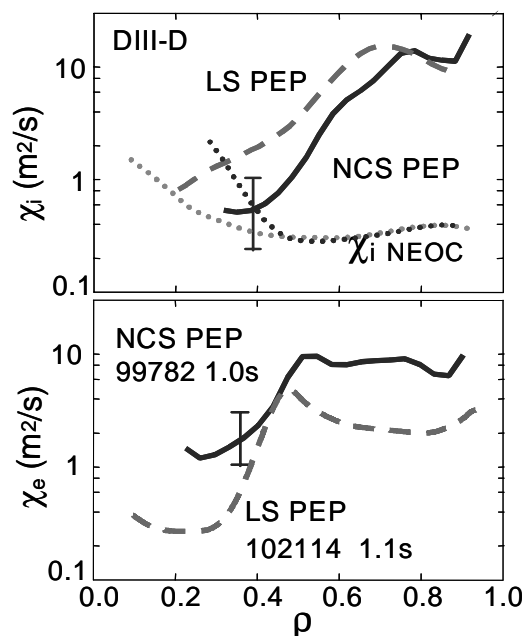


FIG. 5. Transport analysis results for NCS PEP discharge (solid) and LS PEP discharge (dashed) showing ion thermal diffusivity and electron thermal diffusivity.

The core pressure is diminished immediately with the onset of MHD activity that is coincident with the q profile passing through low order rational values. Methods to keep q above 2 across the entire profile to avoid such a termination are under evaluation.

PEP ITBs have been investigated in different magnetic shear and NBI configurations. We find the lowest ion thermal transport in strongly NCS plasmas with high power counter-NBI where E_r is the strongest since the pressure gradient and toroidal rotation components add in the same direction. This configuration yields the strongest $\mathbf{E} \times \mathbf{B}$ shearing rate that is believed responsible for ion temperature gradient (ITG) mode stabilization [1,9]. With a monotonic q -profile it is possible to obtain a peaked density plasma with HFS pellet injection that has a weaker ion transport barrier than the 11 MW NCS high input torque case as shown in Fig. 4. Transport analysis with TRANSP is shown in Fig. 5 for the NCS PEP and a 5 MW co-NBI LS PEP case at the time of peak performance. The ion thermal conductivity is lower in the NCS PEP case presumably because the $\mathbf{E} \times \mathbf{B}$ shearing rate is high while it is very low in the LS PEP case. The electron transport barrier is strong in the LS case showing that the electron barrier is not directly driven by the ion performance. The good electron thermal transport in the core where the density is greatest suggests that high density may be related to the reduction in the anomalous electron transport.

The pellets injected from the different locations have also been used to modify plasma edge conditions to investigate H-mode transitions and edge localized mode (ELM) interaction. Pellets injected from the different locations have been observed to directly produce L-mode to H-mode transitions [10]. An example of this transition for a pellet injected from the HFS45 port is shown in Fig. 6. These transitions have been produced as a result of a significant increase in edge electron density with lower edge electron and ion temperatures. This implies that a critical edge temperature is not required for the H-mode transition since the pellets significantly lower the edge temperature. The radial extent of the

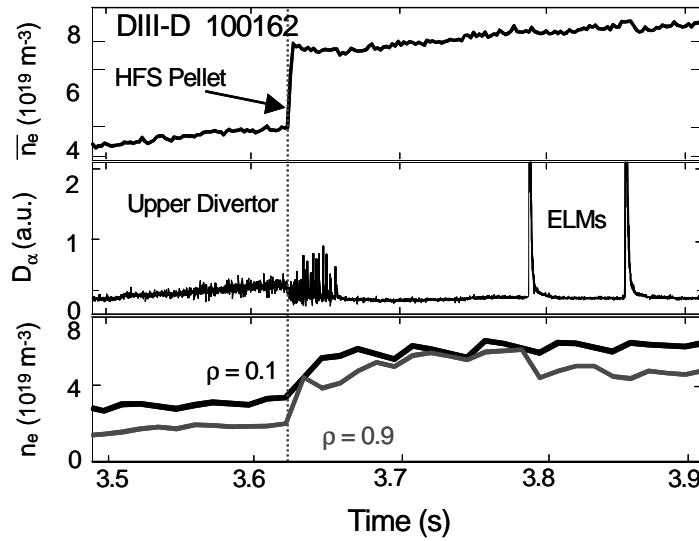


FIG. 6. Evolution of a 4.8MW NBI discharge with a HFS pellet injected that triggers an L-mode to H-mode transition. Dithering in the divertor D_α is observed just before the transition.

pellet mass deposition is not important, as pellets from the LFS, HFS 45 and V+3 ports have all triggered the transitions with significantly different deposition profiles. Pellet injection from all locations produces a steep edge electron density gradient. A critical edge density gradient on the order of $1 \times 10^{21} \text{m}^{-4}$ is required to trigger the transition independent of the injection location. The plasma edge parameters are well below those required by several analytic theoretical models of the transition [10] thus suggesting that further theoretical work is required to understand the transition mechanism. In these DIII-D experiments the power required to access the H-mode was reduced by as much as 30%.

4. Summary

Pellets injected from inside the magnetic axis from the inner wall or vertical port leads to stronger central mass deposition than pellets injected from the outside midplane and thus yield deeper more efficient fueling. These ports take advantage of a major radius drift of the pellet mass that deposits particles deeper into the plasma than the pellet travels. The HFS ports have been used to deposit central mass that forms a transport barrier in the plasma core when heated with either co- or counter-NBI. These ITBs are formed with low or negative central shear and have highly peaked density profiles with $T_e \sim T_i$. The reduced ion transport in the ITB is consistent with $\mathbf{E} \times \mathbf{B}$ shear suppression of ITG modes. Pellets from all injection locations have been used to trigger L-mode to H-mode transitions. These transitions effectively lower the H-mode power threshold by as much as 30%. The transition does not require a critical edge temperature, but does require a critical edge density gradient on the order of $1 \times 10^{21} \text{m}^{-4}$, independent of the pellet injection location. Pellet injection from the different injection ports has proved to be a useful tool for providing new physics understanding on DIII-D.

Acknowledgements

The authors would like to acknowledge the support and encouragement of Drs. S. L. Milora, P. K. Mioduszewski, R. D. Stambaugh, and T. S. Taylor. This work was supported by the Oak Ridge National Laboratory managed by UT-Battelle, LLC, for the U.S. Department of Energy under Contract No. DE-AC05-00OR22725 and also supported under contracts DE-AC03-99ER54463, DE-AC02-76CH03073, and DE-FC02-99ER54512.

References

- [1] BAYLOR, L.R., et al., Phys. Plasmas **7** (2000) 1878.
- [2] LANG, P.T. et al, Phys. Rev. Lett. **79** (1997) 1478.
- [3] PARKS, P.B., Sessions, W.D, Baylor, L.R., Phys. Plasmas **7** (2000) 1968.
- [4] BAYLOR, L.R., et al., accepted for publication in J. Nucl. Mater.
- [5] FERRON, J.R., et al., Phys. Plasmas **7** (2000) 1976.
- [6] The JET Team (G.L. Schmidt), Plasma Physics and Controlled Nuclear Fusion Research, (Proc. 12th Int. Conf. Nice, 1988), IAEA Vienna, 215 (1989).
- [7] GREENFIELD, C.M., et al., Phys. Plasmas **7** (2000) 1959.
- [8] DOYLE, E.J., et al., these proceedings.
- [9] BURRELL, K.H., Phys. Plasmas **4** (1997) 1499.
- [10] GOHIL, P., et al., submitted to Phys. Rev. Lett.